
CREEPING INSIGHTS: A DEEP DIVE INTO THE BEHAVIOR AND MODELS OF XIAPA LANDSLIDE'S SLIDING ZONE SOILS

Mei Yilin, Shi Xuanzhe and Deng Chengxi

¹State Key Laboratory of Hydraulics and Mountain River Engineering, School of Water Resources and Hydropower, Sichuan University, Chengdu, Sichuan, 610065, China

²Sichuan Electric Power Design Consulting Co., Ltd., Chengdu, Sichuan, 610041, China

Abstract

To study the creep properties of the sliding zone soils, the triaxial creep tests under different confining pressures and stress levels were performed. The confining pressures ranged from 100 kPa to 400 kPa, and the stress levels ranged from 0.30 to 0.75 for each confining pressure. Results indicated that the sliding zone soils exists obvious creep behavior. The axial strain increases with time, and the axial strain growth rate gradually decreases with time and eventually tends to a stable value. The creep process can divide into the instantaneous deformation phase, decay creep phase and steady creep phase. An empirical creep model was presented to describe the stress-strain-time of the sliding zone soils. The model calculation results have a good relationship with the test data. The empirical creep model can describe the creep rule of the sliding zone soils.

Keywords: sliding zone soils, creep, triaxial test, creep model

1. Introduction

Ancient landslides are landslides that have occurred in the past and remain relatively stable for a long period of time [1,2,3]. The time-dependent stress and deformation of the ancient landslides causing by the creep behavior of sliding zone result in the instability of slopes. The sliding zone is a relatively weak zone in ancient landslides and the sliding zone soils are gravel - clay mixtures. Therefore, it is necessary to study the creep behavior of the sliding zone soils [4,5,6].

Many researchers have studied on the creep behavior of the sliding zone soils. Tan [7] carried out the in-situ triaxial creep test and the large-scale direct shear test in laboratory for the sliding zone soils. Test results showed that the creep of the sliding zone soils in the in-situ test is decay creep, and the sample is not been visibly damaged although the creep deformation increases with the increase in time. Chen [8] carried out the shear creep test of the sliding zone soils under different loading conditions. Test results showed that the shear creep of the sliding zone soils is greatly affected by the stress path and the void ratio after loading. Based on the unsaturated triaxial creep test, Lai [9] found that the creep and creep rate increase with the decrease in the matrix suction under the same deviator stress. At the same time, the deviator stress increases, the final creep increases, and the effect extent of the deviator stress is greater than the matrix suction. Many researchers have presented creep empirical models to study

the creep properties and rules of the sliding zone soils [10,11,12]. Mesri model, Singh-Mitchell model and Burgers model are widely used. However, Singh-Mitchell model had a poor prediction at low stress levels. Burgers model is a Maxwell model and a Kelvin model in series, and ignored the effect of plastic strain. Mesri model had a better fitting at all stress levels [13]. Stress level and confining pressure affect the creep of the sliding zone soils mainly. Many researches have been made on creep of slopes, and there is a few studies on the creep of the sliding zone soils of the ancient landslides.

In this paper, the triaxial creep tests under different confining pressures and stress levels is carried out to study the creep characteristics of the sliding zone soils of Xiapa landslide at Jinping I Hydropower Station. The creep law and the empirical creep model were presented.

2. Triaxial creep test of the sliding zone soils

Xiapa landslide is located in the reservoir area of Jinping I Hydropower Station. It is an ancient landslide with the area of 0.45km². The soil sample is a borehole soil with the depth of 63.0m~76.9m, dry density $\rho_d=1.92$ g/cm³ and water content $w=15.0\%$. The specific gravity $G_s=2.75$, liquid limit $w_L=33.0\%$, plastic limit $w_P=18.6\%$ and plasticity index $I_p=14.4$. The content of clay is 18.2%, and the grading curve is shown in Figure 1. The cohesion $c=75$ kPa and the internal friction angle $\varphi=25.9^\circ$ according to the consolidated-drained triaxial compression test.

The consolidated-drained triaxial creep tests are carried out by using the triaxial creep apparatus. The confining pressures σ_3 are 100, 200, 300, and 400 kPa. The stress levels s is 0.30, 0.45, 0.60 and 0.75 for each confining pressure. The stress level is the ratio of the deviator stress to the failure deviator stress. The sample is a cylindrical one with the diameter of 101 mm and height of 200 mm. The dry density ρ_d and the water content w of sample are 1.92 g/cm³ and 15.0%, respectively. The sample was compacted in five layers according to the dry density and water content to ensure the uniformity of the sample. The sample was consolidated with the time of 24h. The loading method is step loading, and the loading process is finished within 1 minute. During the test, calculate the cross-sectional area of the sample according to the axial and volume deformation, and adjust the axial loading in time to ensure the constant axial stress. Test is finished when the ratio of deformation in 24h to total deformation is less than 0.005 [14]. The temperature of water in the laboratory is 15~20°C.

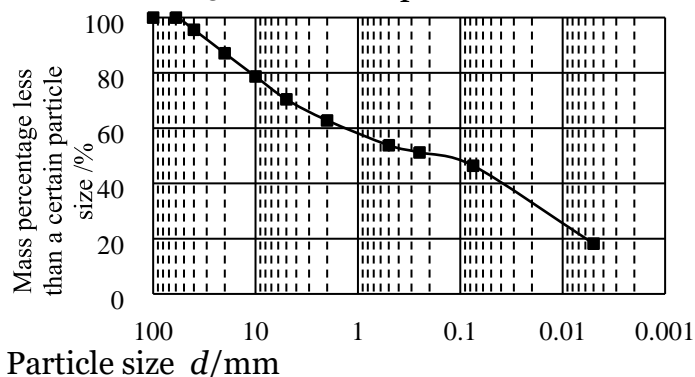


Figure 1: Gradation curve of the sliding zone soils

3. Test results and analyses

3.1. Axial strain-time behavior

Test results are processed according to the Boltzmann linear principle. The axial strain ε_a -time t curves were shown in Figure 2, taking $\sigma_3=300$ kPa as an example. It can be seen that the sliding zone soils have obvious creep behavior. The axial strain increases with the increase in time, and the growth rate gradually decreases and finally reaches a stable value.

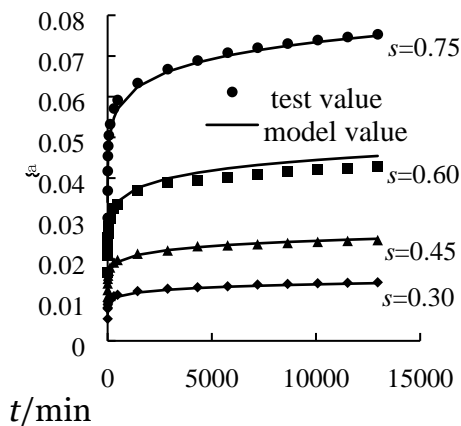


Figure 2: Axial strain ε_a -time t curves ($\sigma_3=300$ kPa)

3.2. Deviator stress- axial strain behavior

The stress-strain curves of the sliding zone soils were shown in Figure 3, taking $\sigma_3=300$ kPa as an example. It can be seen that the stress-strain curves are strain-hardening. The non-linear characteristics gradually become obvious with the increasing of time, indicating that the deformation of the sliding zone soils has a time effect.

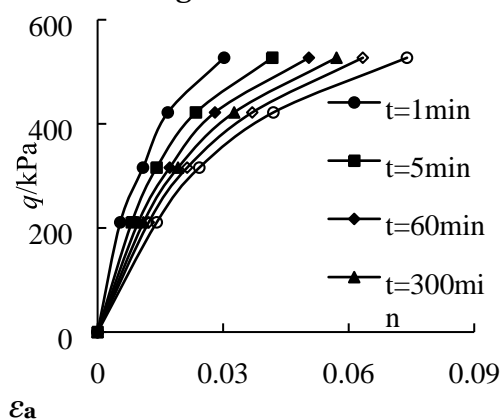


Figure 3: Stress q -strain ε_a curves ($\sigma_3=300$ kPa)

3.3. Stress-strain-time behavior

3.3.1. Strain-time relationship

The strain-time relationship can use power function, logarithmic function and exponential function^[13]. Since the power function is in good agreement with the experimental data, the power function was used to express the strain-time relationship, namely:

$$\varepsilon_a = n t^m$$

$$\varepsilon_a = \varepsilon_{ar} \left(\frac{t}{t_r} \right)^n \quad (1)$$

$$\lg \varepsilon_a = \lg \varepsilon_{ar} + n \lg \left(\frac{t}{t_r} \right) \quad (2)$$

Where: ε_a is the axial strain, t_r is the reference time, and $t_r = 1$ min; ε_{ar} is the reference axial strain under the reference time; n is the material parameter.

Logarithmic transformation is used for equation (1), we get

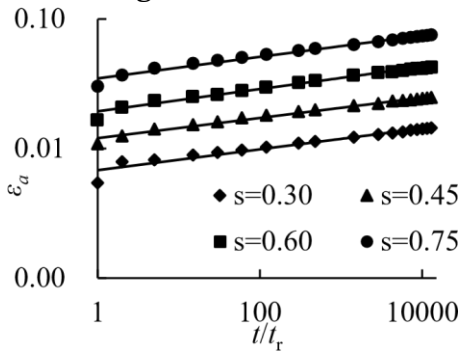
$$\lg \varepsilon_a = \lg \varepsilon_{ar} + n \lg \left(\frac{t}{t_r} \right) \quad (2)$$

$$\lg \varepsilon_a - \lg \varepsilon_{ar} = n \lg \left(\frac{t}{t_r} \right)$$

$$\lg \varepsilon_a - \lg \varepsilon_{ar} = n \lg \left(\frac{t}{t_r} \right)$$

According to equation (2), the power exponent n is the slope of $\lg \varepsilon_a - \lg \left(\frac{t}{t_r} \right)$ curve, as shown in Figure 4.

Figure 4, taking $\sigma_3 = 300$ kPa as an example. The values of n under different confining pressures and deviator stress levels were shown in Table 1. The maximum and minimum values of the n are 0.0925 and 0.062, respectively. The values of n have small difference for the tested sliding zone soils so that the average value is taken to as the value of n .



$$\lg \varepsilon_a - \lg \left(\frac{t}{t_r} \right) = n \lg \left(\frac{t}{t_r} \right)$$

Figure 4: $\lg \varepsilon_a - \lg \left(\frac{t}{t_r} \right)$ curves ($\sigma_3 = 300$ kPa)

Table 1: Parameter values of power function empirical creep model of the sliding zone soils.

Numble	ε_{ar}	q/kPa	q_f/kPa	n	R^2	a_{ar}	b_{ar}	R^2
T1-0.30	0.00496	118		0.0723	0.997			
T1-0.45	0.00894	177		0.0925	0.961			
T1-0.60	0.01882	236	393	0.0666	0.999	0.0118	0.9708	0.993
T1-0.75	0.03087	296		0.0696	0.998			
T2-0.30	0.00490	164		0.0811	0.98			
T2-0.45	0.00766	247		0.0883	0.963			
T2-0.60	0.01595	329	546	0.0882	0.953	0.0106	0.9939	0.996
T2-0.75	0.03137	411		0.0842	0.958			

T3-0.30	0.00683	211		0.0806	0.942			
T3-0.45	0.01187	316		0.0781	0.983			
T3-0.60	0.01940	422	703	0.0859	0.977	0.0164	0.8524	0.998
T3-0.75	0.03485	527		0.0832	0.977			
T4-0.30	0.00885	257		0.062	0.985			
T4-0.45	0.01357	386		0.0796	0.985			
T4-0.60	0.02447	514	857	0.0717	0.985	0.0209	0.8112	0.987
T4-0.75	0.04043	643		0.0792	0.996			

^a1 represents the confining pressure of 100 kPa. ^b0.30 represents the stress level, and the other numbers can be deduced by analogy.

3.3.2. Stress-strain relationship

The stress-strain relationship can fit by the exponential function and hyperbolic function. Since the hyperbolic function is in good agreement with the experimental data, so the hyperbolic function form is adopted:

$$s a_{ar} \epsilon_{ar} = 1 - s b_{ar} \quad (3)$$

Where, ϵ_{ar} is the reference axial strain, s is the stress level, and a_{ar} and b_{ar} are model parameters. In order to obtain the model parameters a_{ar} and b_{ar} , the equation (3.3) is rewritten as,

$\epsilon_{ar} = b_{ar} \epsilon_{ar} a_{ar} s \quad (4)$

The model parameters a_{ar} and b_{ar} are the intercept and slope ratio of $-\epsilon_{ar}$ curve, respectively. s

The $-\epsilon_{ar}$ curves were shown in Figure 5, Taking $\sigma_3=300$ kPa as an example. The values of the a_{ar} s and b_{ar} under different confining pressures were shown in Table 1.

The $-\epsilon_{ar}$ curves were shown in Figure 5, Taking $\sigma_3=300$ kPa as an example. The values of the a_{ar} s and b_{ar} under different confining pressures were shown in Table 1.

The $-\epsilon_{ar}$ curves were shown in Figure 5, Taking $\sigma_3=300$ kPa as an example. The values of the a_{ar} s and b_{ar} under different confining pressures were shown in Table 1.

The $-\epsilon_{ar}$ curves were shown in Figure 5, Taking $\sigma_3=300$ kPa as an example. The values of the a_{ar} s and b_{ar} under different confining pressures were shown in Table 1.

The $-\epsilon_{ar}$ curves were shown in Figure 5, Taking $\sigma_3=300$ kPa as an example. The values of the a_{ar} s and b_{ar} under different confining pressures were shown in Table 1.

The $-\epsilon_{ar}$ curves were shown in Figure 5, Taking $\sigma_3=300$ kPa as an example. The values of the a_{ar} s and b_{ar} under different confining pressures were shown in Table 1.

The $-\epsilon_{ar}$ curves were shown in Figure 5, Taking $\sigma_3=300$ kPa as an example. The values of the a_{ar} s and b_{ar} under different confining pressures were shown in Table 1.

The $-\epsilon_{ar}$ curves were shown in Figure 5, Taking $\sigma_3=300$ kPa as an example. The values of the a_{ar} s and b_{ar} under different confining pressures were shown in Table 1.

The $-\epsilon_{ar}$ curves were shown in Figure 5, Taking $\sigma_3=300$ kPa as an example. The values of the a_{ar} s and b_{ar} under different confining pressures were shown in Table 1.

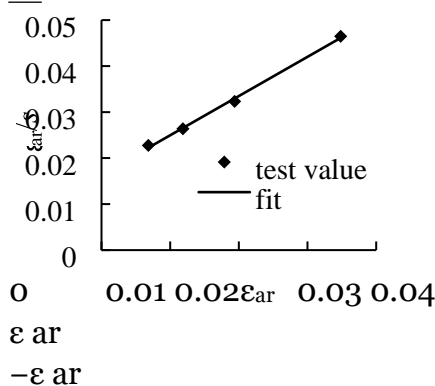


Figure 5: σ curves ($\sigma_3=300$ kPa)

3.3.3. Empirical creep model

Substituting equation (3) into equation (1), an empirical creep model for the sliding zone soils can be obtained, namely:

$$\varepsilon_a = \frac{1}{n} \left(\frac{\sigma_a}{\sigma_{ar}} \right)^n \left(1 - \frac{\sigma_a}{\sigma_{ar}} \right) t^{\frac{1}{n}} \quad (5)$$

In order to verify the reliability of the empirical creep model, the comparison between the model values and the test value was given, as shown in Figure 2. It can be seen that the trend of the calculated results is consistent with that of the test data, and the difference of values are small. Using the empirical creep model to describe the creep behavior of the sliding zone soils is feasible.

4. Conclusion

The triaxial creep tests were carried out for the sliding zone soils in the Xiapa landslide. The creep law of axial strain is analysed and an empirical creep model was presented. The main conclusions are as follows:

- (1) There exists obvious creep behavior for the sliding zone soils in the Xiapa landslide. The axial strain increases with time, and the axial strain growth rate gradually decreases with time and eventually tends to a stable value. The entire deformation stage can be divided into the instantaneous deformation phase, decay creep phase and steady creep phase.
- (2) The strain-time relationship and stress-strain relationship of the sliding zone soils can be simulated by power function and hyperbolic function, respectively, and the empirical creep model of the sliding zone soils is given; the model calculation results have a good relationship with the test values. The empirical creep model can describe the creep rule of the sliding zone soils.

References

- Zhang S Y. Importance of geological survey in the hydropower project of metal mine[J]. World Nonferrous Metals, 2016.
- Zhang Y S, Wu R A and Guo C B. 2018 Research progress and prospects of the resurrection of ancient landslides, J. Advances in Earth Science. 33(2018)728-40
- Li Y F and Ji Q W. 2006 Discussion on the identification of ancient landslides, J. West-China Exploration Engineering. 12(2006)286-7
- Liu X L, Deng J H and Li G T. 2004 Research status of strength characteristics of sliding zone soil, J. Rock and Soil Mechanics. 25(2004)1849-54
- Zhou J J, Zhao F S and Yuan X Q. 2020 Analysis of creep process and microstructure evolution of sliding zone soil, J. Hydrogeology & Engineering Geology. 47(2020)115-21

- Sun M J, Tang H M and Wang X H. 2017 Study on creep characteristics of soil in creeping landslide, J. Rock and Soil Mechanics. 38(2017)385-91
- Tan Q W. 2019 Research and application of sliding zone soil characteristics based on in-situ creep test (Wuhan: China University of Geosciences)
- Chen Q, Cui D S, Wang J E. 2020 Creep test study on the sliding zone soil of Huangtupo landslide under different consolidation states, J. Rock and Soil Mechanics. 41(2020)1635-42
- Lai X L, Ye W M and Wang S M. 2012 Experimental study on unsaturated creep characteristics of landslide soil, J. Chinese Journal of Geotechnical Engineering. 34(2012)286-93
- Long J H, Guo W B and Li P. 2010 Creep characteristics of sliding zone soil in loess landslide, J. Chinese Journal of Geotechnical Engineering. 32(2010)1023-28
- Wang B, Zhu J B and Tang H M. 2008 Research on the creep characteristics of soil in the sliding zone of Huangtupo landslide, J. Journal of Yangtze River Scientific Research Institute. 25(2008)49-52 [12] Wang C, Hu D J and Liu H W. 2003 Experimental study on the creep of the sliding zone soil of the Xietan landslide in the Three Gorges, J. Rock and Soil Mechanics. 24(2003)1007-10
- Lin H D and Wang C C. 1998 Stress-strain-time function of clay, J. Journal of Geotechnical and Geoenvironmental Engineering, America Society of Civil Engineering. 124(1998)289-96
- Ministry of Housing and Urban-Rural Development of the People's Republic of China, State Administration for Market Regulation. Standard for Geotechnical Testing Method: GB/T 50123-2019. (Beijing: China Planning Press)